Earthquake Geotechnical Engineering for Protection and Development of Environment and Constructions – Silvestri & Moraci (Eds)
© 2019 Associazione Geotecnica Italiana, Rome, Italy, ISBN 978-0-367-14328-2

Investigation of post-failure axial capacity of lightly reinforced concrete piles

V. Drosos
GR8 GEO, Athens, Greece (formerly: Fugro)

A. Papageorgiou
STRUSUS Consulting, Rhodes, Greece

A. Giannakou & J. Chacko
GR8 GEO, Athens, Greece (formerly: Fugro)

S. De Wit
Shell Global Solutions International B. V., Rijswijk, the Netherlands

ABSTRACT: Occurrence of man-induced earthquakes in areas of low tectonic seismicity, where most structures have not been designed to resist earthquake loading, created the need for seismic performance evaluation of existing structures. Evaluations performed revealed that in some cases seismic demands on existing structures and their foundations may be larger than the available capacity and therefore a retrofit scheme is often proposed and designed. This paper presents a numerical study in order to investigate whether a pile whose shear structural capacity has been exceeded is still able to carry the vertical loads of the superstructure following an earthquake. A methodology useful for the preliminary seismic evaluation of poorly reinforced pile foundations was developed that is based on analytical models developed for lightly reinforced columns. Analysis of a case-study from northern Europe using the proposed methodology showed that piles can bear vertical loads even after shear failure has initiated, as long as the imposed drifts on the pile are less than a critical value. For most of the cases analyzed, the pile fails in shear, but appears to continue to carry the vertical loads. This finding is likely to have a significant influence on the design of retrofit approaches.

1 INTRODUCTION

Retrofit of the foundation (and especially of a pile foundation) is an expensive and cumbersome task. It is for this reason that in seismic areas piles are designed to remain elastic following a design earthquake and nonlinearity is typically allowed in the superstructure where inspection, repair, and retrofit can occur relatively easily. Nevertheless, several case-histories (especially from the Kobe 1995 earthquake in Japan) have shown that pile yielding under strong shaking cannot be avoided, especially for piles embedded in soft soils. Pile yielding is also probable in existing piles that have not been designed to resist seismic loads and are therefore lightly reinforced subjected to man-induced seismicity. However, a number of cases have been reported indicating that piles continue to bear the vertical loads of a building, preventing collapse, even when they have sustained severe cracking due to shear or bending capacity exceedance. The most characteristic of these cases is the NHK Building in Niigata, Japan. Despite the failure in shear due to liquefaction of the coarse-grained soil during the Niigata earthquake in 1964, interestingly, the pile yielding was only identified 20 years after the earthquake when the soil was excavated for a new project construction. During this 20-year period the building was in service despite the hidden shear failure of the piles.

Although direct extrapolation of this experience cannot be applied to areas of very low tectonic seismicity, such as those encountered in northern Europe, since the detailing of existing piles in there does not resemble that used in earthquake prone regions, it may still be possible that existing lightly-reinforced concrete piles provide sufficient vertical capacity to prevent collapse, even when the seismic demand exceeds the estimated/assumed shear and/or bending capacity of the pile.

A numerical study was undertaken with the goal to investigate whether a pile whose shear structural capacity has been exceeded is still able to carry the vertical loads of the superstructure following an earthquake. Considering the limited information/research available on the post-failure behavior of reinforced concrete piles and given that the structural function of a pile resembles that of a column, the relative literature on post-failure capacity of columns provides the best available source of knowledge on the topic.

2 POST-FAILURE BEHAVIOR OF COLUMNS AND PILES

Despite the structural resemblance of piles to columns, the presence of soil differentiates the response of the pile from that of a column. The role of the soil is twofold: it may apply additional loads on the pile due to kinematic interaction, but at the same time, it may provide an extra confinement to the concrete of the pile increasing its ductility thus improving the post-failure behavior. Maki and Mutsuyoshi (2004) and Mohammed and Maekawa (2012) explored the impact of soil confinement on the behavior of the piles and concluded that soil confinement around plastic hinges restrain the spalling of cover concrete and local buckling of reinforcement, hence increasing the pile ductility. The effect of soil confinement diminishes close to the pile head.

While research on the post-failure behavior of reinforced concrete piles is very limited, several researchers have studied the post-failure axial capacity of reinforced concrete columns (e.g. Yoshimura and Yamanaka, 2000; Shirai et al., 2001; Sezen, 2002; Elwood and Moehle, 2003). Ex-periments have shown that the lateral capacity of a poorly-reinforced column after failure degrades to a small residual value. This has a major effect on the axial capacity of the column. Based on the experimental results, researchers have drawn the following key conclusions: a) axial failure occurs when the shear capacity of the structural member reduces to almost zero; b) drift at axial failure decreases with increasing axial load; and c) columns with smaller hoop spacing can bear the vertical load at larger drifts compared to columns with larger hoop spacing.

3 ANALYTICAL MODEL USED FOR THE NUMERICAL SIMULATION OF POST-FAILURE BEHAVIOR OF PILES

The empirical model proposed by Elwood and Moehle (2003) to estimate the drift at shear and at axial failure of existing lightly-reinforced concrete columns was used to develop a methodology for the preliminary seismic evaluation of poorly reinforced pile foundations. According to this model, the behavior of a poorly reinforced column can be idealized with the backbone curve presented in Figure 1a. Four regimes are identified: a) at the beginning the structural member deforms almost linearly with the initial stiffness up to the point where yielding occurs (δ_y); b) the column reaches the ultimate lateral capacity (V_u) and it continues deforming up to a drift δ_s which denotes failure in shearing and formation of a shear crack; c) for larger deformations, the lateral capacity of the column reduces as the column cross-section further disintegrates; d) at the point where lateral capacity reduces to almost zero (δ_a) the column starts losing its axial capacity as well. After this point, and if the drift continues increasing, the axial capacity of the column degrades according to a limit curve as shown in Figure 1b.

Elwood and Moehle (2003) provided the following empirical equation for the estimation of the drift at shear failure δ_s [= Δ_s/L].

$$\left(\frac{\Delta_s}{L}\right) = \frac{3}{100} + 4\rho'' - \frac{1}{40}\frac{\nu}{\sqrt{f_c'}} - \frac{1}{40}\frac{P}{A_g f_c'}\frac{1}{100}(\textit{units in MPa}) \quad (1)$$

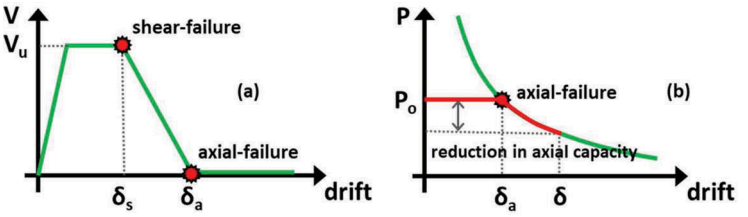

Figure 1. Idealized behavior of a lightly-reinforced column according to Elwood and Moehle (2003).

where ρ'' is the transverse reinforcement ratio defined as the cross-sectional area of the transverse reinforcement over the product of the column width b and hoop spacing s (A_{st} / bs), f'_c is the concrete compressive strength, P is the axial load, A_g is the gross cross-sectional area of the column, and v is the nominal shear stress (V / bd). In accordance with experimental data, the model suggests that the drift to denote shear failure increases with more transverse reinforcement and decreases with increasing axial load.

For the estimation of the drift at axial failure (δ_a), Elwood and Moehle (2003) developed a simplified shear-friction model and calibrated it using experimental data. For a damaged column with the characteristic diagonal crack developed, any axial load supported by this column must be transferred across the crack. The load that can be transferred across the crack is a function of the normal stress on the failure surface. Reviewing the experimental data, Elwood and Moehle empirically determined the equation for the estimation of the drift at axial failure δ_a [= $(\Delta/L)_{axial}$].

$$\left(\frac{\Delta}{L}\right)_{axial} = \frac{4}{100}\frac{1+tan^2\theta}{tan\theta + P\left(\frac{s}{A_{st}f_{yt}d_c tan\theta}\right)} \tag{2}$$

where θ is the angle of the crack relative to the horizontal (typically 65°), f_{yt} is the steel yield strength, and d_c is the depth of the column core from center line to center line of the ties.

Having developed empirical models for the assessment of the drift at shear (δ_s) and at axial (δ_a) failure, Elwood and Moehle (2003) developed a macro-element to describe the behavior of lightly reinforced columns. The model of the shear-critical column consists of three elements. A nonlinear beam element models the flexural nonlinear behavior of the column. A shear spring is added on top of the column (in series) to simulate the behavior of the column in shear according to the model by Elwood and Moehle (2003). Finally, one more spring is added in series to simulate the axial behavior of the column after failure.

According to Elwood and Moehle (2003) recommendations, the behavior of the shear spring is defined by a trilinear relationship. The first branch of the envelope describes the shear behavior of the column before failure. It is defined by the initial stiffness which can be approximated by the shear stiffness of the column, $K_{ini} = GA/L$. This initial segment of the envelope continues until the shear load reaches the shear capacity of the column, V_o or the drift at shear failure, δ_s, whatever comes first. At this point, the second branch of the response starts with a negative stiffness, K_{deg}. This negative stiffness can be determined as follows:

$$K_{deg} = \left(\frac{1}{K^t_{deg}} - \frac{1}{K_{unload}}\right)^{-1} \tag{3}$$

where K_{unload} is the unloading stiffness of the beam element (flexural response) —which is usually taken equal to the initial loading stiffness of the beam, and K^t_{deg} the (negative) stiffness of the resultant response (beam + shear spring) and is determined from the line connecting the point of shear failure (δ_s, V_o) and the drift at axial failure, δ_a (δ_a, *0*). Finally, the third branch of the response envelope is defined by the residual shear capacity of the column, V_{res} (typically assumed equal to 15% of the ultimate shear capacity according to seismic codes).

The empirical model described above was implemented in the finite element software OpenSees (Mazzoni et al., 2010) to be used for the numerical simulations of lightly-reinforced piles under seismic loading. The uniaxial hysteretic material *Pinching4* (Lowes et al., 2004) was selected from the OpenSees material library to simulate the shear behavior of a lightly reinforced pile elements (shear spring). *Pinching4* is a general one-dimensional hysteretic load-deformation relationship that can be calibrated to represent the response of a structural member under monotonic or cyclic loading. The constitutive relationship includes a response envelope, an unload-reload path, and three optional damage rules that control the evolution of the response. The response envelope and the unloading-reloading path are defined as multilinear relationships and thus the model is able to describe rather complicated hysteretic loops. The axial spring proposed by Elwood and Mohle (2003) for modeling the axial capacity degradation after failure was omitted, conservatively assuming that pile loses all its axial capacity as soon as the drift at axial failure is reached.

We note that the macro-element developed by Elwood and Moehle (2003) for lightly reinforced columns (i.e. *LimitState* material in OpenSees material library) could not be readily implemented for the simulation of pile behavior since the pile needed to be discretized into a series of elements with connected soil springs that model the nonlinear soil-pile interaction behavior with depth.

4 MODEL VALIDATION

Due to lack of experiments on the post-axial failure capacity of lightly reinforced piles, the model was validated against shake table tests performed by Elwood and Moehle (2003) that investigated the dynamic response of shear-critical columns and their post-failure axial capacity. A frame consisting of three columns with the central one designed to be shear-critical (wider spacing of transverse reinforcement) was tested. Details of the experiment are provided in Elwood and Moehle (2003). Using the finite-element code OpenSees and the analytical model described above, the shake table experiment was modeled in order to validate the analytical model. The *Pinching4* material was calibrated for the experiment following the procedure described earlier.

The results of the numerical analysis of the experiment are compared with the measured response of the central column in Figure 2. The shear force – horizontal displacement hysteretic loops illustrate that the numerical model is able to reproduce efficiently all the components of the column behavior: the initial stiffness of the column, the ultimate shear capacity, the strength degradation and the residual strength, and the unloading stiffness. The calculated response of the column is bounded by the backbone curve defined from a push-over analysis. The numerical model has predicted sufficiently the shear force variation with time/displacement and the characteristic points of shear and axial failure are clearly identified at about the same point as in the experiment.

5 NUMERICAL INVESTIGATION OF POST-FAILURE BEHAVIOR OF LIGHTLY REINFORCED PILES

5.1 *Approach*

For the numerical investigation of post-failure behavior of lightly reinforced piles a 2-story building located in northern Europe was selected as a case study. The building is constructed of precast concrete wall elements and steel frames supporting the slabs with a foundation consisting of cast in-situ foundation beams supported on concrete bored piles. One pile from this building was se-lected for application of the proposed methodology.

The pile was modeled as a beam-on-nonlinear-Winkler foundation (BNWF). The pile elements were connected to the soil through a set of springs simulating the soil-pile interface behavior (i.e. p-y and t-z springs based on the soil deposit properties and using API (2000) recommendations). The free ends of the springs were excited by the free-field soil motion at the corresponding depth. A one-dimensional site response analysis performed separately to calculate the free-field motion at these depths. The inertial loads imposed to the foundation

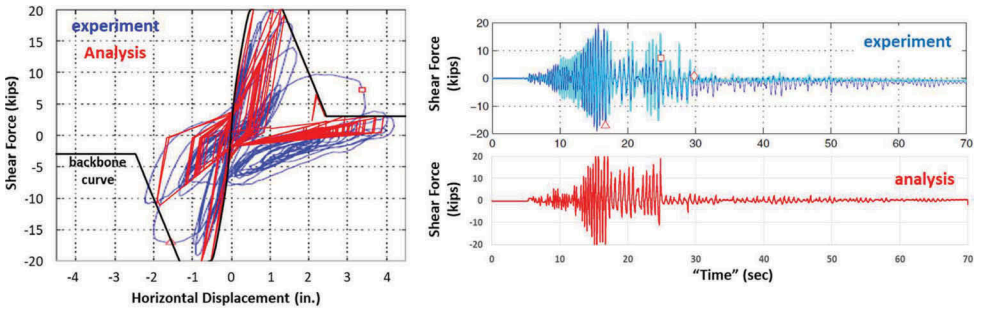

Figure 2. Analysis results vs. experiment measurements of the response of the central column to horizontal cyclic load. Hysteretic loops of shear force against horizontal relative displacement (the idealized backbone curve [black line] according to the empirical model by Elwood and Moehle is superimposed) and shear force time histories

by the oscillation of the superstructure were considered in a simplified manner (i.e. through a 1-dof oscillator added above the pile head with a fundamental fixed-base period of 0.3 s).

Shear springs following Elwood and Moehle's model were added between consecutive beam elements at locations where significant shear forces were expected to develop and shear failure was likely to occur. To identify locations of substantial shearing, an analysis considering the pile with infinite shear capacity was conducted first. Shear springs were then placed at the location of these critical points and analyses were repeated.

5.2 *Development of Free-Field Time Histories Along Pile*

The soil profile consists of a thick layer of soft clay (about 9 m thick) overlying an approximately 3-m thick medium dense sand layer. A clay layer of 1 m thickness is encountered between the medium dense sand layer and a deeper dense sand layer that was present to the maximum depth explored (about 23 m depth). Figure 3 illustrates the stratigraphy of the idealized soil profile and presents the interpreted shear wave velocity (V_s) profile. Following the applicable seismic code provisions, the input motion was applied at a stiff-soil horizon with shear wave velocity of 300 m/s which was encountered at 22.5 m depth.

Nonlinear site response analyses were performed to develop free-field soil motion along the pile that were applied at the free end of the p-y springs. Since no site-specific dynamic laboratory tests are available for the site, Darendeli's (2001) modulus reduction and damping curves were used. For the clay layers a plasticity index (PI) equal to 40 was assumed.

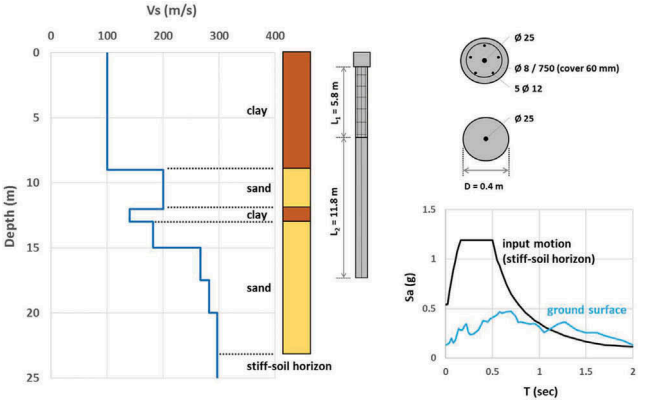

Figure 3. Case study from man-induced seismicityarea in northern Europe: idealized soil profile at the site (left), ground motions (bottom right), and analyzed pile geometry and detailing (top right)

Input motions were derived according to the applicable seismic code that incorporated demands due to man-induced earthquakes resulting in a design PGA value at stiff soil conditions of 0.54 g for 1500-year return period. The response spectrum of the input motion at depth and the ground surface response spectrum are presented in Figure 3. Deamplification was observed due to the nonlinear response of the soft soil deposit. Analysis with an input motion of increased PGA at depth (0.81 g) was also performed to investigate the influence of the rather conservative partial factors recommended by the seismic code when nonlinear time history analyses are performed.

5.3 *Pile Modeling*

The geometry of the pile and the detailing are presented in Figure 3. Material properties provided by the structural engineer have been used in this study. The shear capacity $V_{Rd,c}$ of the upper and the lower part of the pile is 77.2 kN and 59.8 kN, respectively. An axial load of 550 kN has been assumed for the examined pile based on the seismic evaluation of the building.

The pile was modeled with 0.5m-long nonlinear beam elements. For the simulation of the non-linear behavior in bending moments and axial loads the cross-section of the beam is discretized in small areas, called fibers, whose behavior is described by the constitutive law of their material. In this way all the components of the cross-section are modeled in detail (i.e. confined concrete/core, unconfined concrete/cover, and longitudinal reinforcement). Concrete fiber behavior is described using the *Concrete02* material from the OpenSees library and reinforcement behavior is modeled with *Steel02* material. During the analysis the resultant response of the fiber section defines the response of the beam element where the section belongs to. The two material models that describe the pile section behavior (i.e. concrete and steel) were calibrated based on the material properties reported by the structural engineer.

As mentioned above shear springs are placed at locations of substantial shearing. Three critical points of increased shear demands were identified along the pile for the reference motion. These locations are associated with depths where interfaces of significant soil stiffness contrast are encountered (i.e. sand-clay interfaces at about 9 and 12 m depth). A shallower point (~7m depth) was considered also critical due to the increased shear forces. In light of the above, three shear springs were added into the pile model at the specific depths. An additional shear spring was placed at the pile head where the presence of the foundation beam (i.e. fixed-head boundary con-ditions) and the superstructure is likely to impose significant demands on the pile.

5.4 *Calibration of the Shear Springs*

From the analysis performed to identify the critical points, it was concluded that the pile is likely to suffer a pure shear failure (i.e. for shear forces close to the ultimate shear capacity of the pile, the bending moments developed are considerably lower than the moment capacity). Since the shear capacity V_0 is known, the only parameter to be estimated for the calibration of the shear springs is the drift at axial failure, δ_a.

For the upper part of the pile, application of Equation 2 is straightforward. Given the transverse reinforcement of the pile (A_{st} = l0^{-4} m^2, s = 0.75 m, f_{yt} = 550 MPa), and assuming a critical crack angle $\theta = 65°$, an axial load P = 550 kN, and a depth of the pile core d_c = 0.28 m, the drift at axial failure for the upper part of the pile is estimated $(\Delta/L)_{axial,upper}$ □ 1.5%.

For the lower part of the pile, direct application of Equation 2 is not possible since transverse reinforcement does not exist, the spacing s tends to infinity and thus drift at axial failure tends to zero. At this point, we note that Elwood and Moehle (2003) ignored the dowel action of the lon-gitudinal reinforcement in the derivation of Equation 2. The justification for disregarding this action is that spalled cover concrete and hoop wide spacing cannot provide enough resistance for the dowel action to develop. Nonetheless, this is not the case for the central rebar of the pile foundation. The central reinforcement runs along the axis of the pile and has sufficient concrete cover and anchor length to warrant the development of dowel action to some extent. The magnitude of the lateral force that can be provided by the central rebar is limited to the

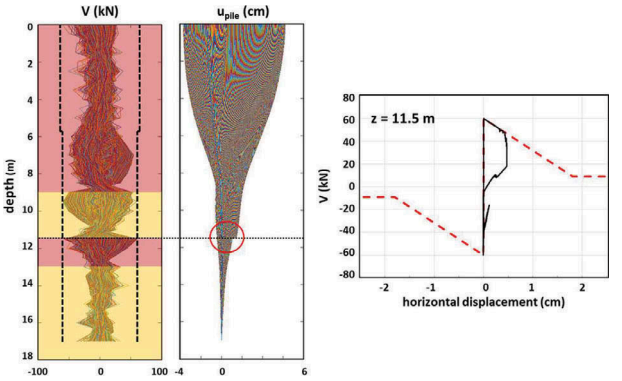

Figure 4. Profiles of shear force (V) and pile relative horizontal displacement (u_{pile}), and hysteretic loop of the pile cross-section at 11.5m depth [red circle marks a critical point with increased shear demands; black dashed line in the shear force plot denotes the shear capacity of the pile; red dashed line denotes the response envelope of the specific pile cross-section]

minimum of the steel bar shear capacity and the dowel action due to concrete resistance. The model proposed by Rasmussen (1963) was used to estimate the dowel action force.

$$V_d = 1.3 d_b^2 \sqrt{f_c f_s} < \frac{A}{\sqrt{3}} f_s \tag{4}$$

where d_b is the rebar diameter, f_c is the concrete compressive strength, f_s is the steel yield strength, and A is the rebar cross-sectional area. To account for cyclic degradation during seismic loading, a partial factor of 2 was applied to V_d (EPPO, 2012).

Rewriting Equation 2 as follows:

$$\left(\frac{\Delta}{L}\right)_{axial} = \frac{4}{100} \frac{1 + tan^2\theta}{tan\theta \frac{P}{F_t}} \tag{5}$$

where F_t is the resisting force provided by the hoops in the free-body diagram, and assuming that this force is provided by the dowel action of the central bar for the lower part of the pile, then the drift at axial failure can be estimated according to Equation 5. From the properties of the central rebar of the pile (d_b = 25 mm, f_s = 550 MPa) and the concrete (f_c = 20 MPa), and assuming a critical crack angle 0 = 65^0, and an axial load P = 550 kN, the drift at axial failure for the lower part of the pile is estimated (A/L) axial, lower — [1]. 7 %.

5.5 *Results*

Figure 4 shows the profiles of shear force (V), pile relative horizontal displacement (u_{pile}), and the shear force – horizontal displacement hysteretic loop of the pile at 11.5 m depth using the reference input motion (PGA = 0.54 g). Each line in the plots corresponds to a specific time during the shaking. The shear capacity is reached only at two points (i.e. 9.5m and 11.5m depth) which indicate the points of shear failure. Indeed, the abrupt change in the pile displacement profile at 11.5m depth [marked with the red circle] reveals the formation of a plastic hinge at this depth. This is better illustrated in the hysteretic loop of the pile at the specific depth. After shear failure the drift continues increasing and the shear force following the backbone curve starts degrading. At a displacement of about 5 mm the seismic motion reverses and the imposed drift reduces again. After this cycle, the seismic motion does not impose larger displacement on the pile and shear capacity does not degrade further. Given that axial failure initiates when the shear capacity reduces to almost zero, it is concluded that the pile is unlikely to lose its axial capacity under this seismic load. Figure 5 shows analysis results for

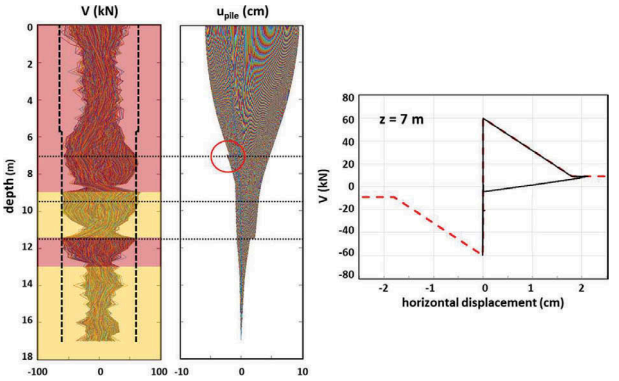

Figure 5. Profiles of shear force (V) and pile relative horizontal displacement (u_{pile}), and hysteretic loop of the pile cross-section at 7m depth

the highest input motion considered with a PGA of 0.81 g. Shear capacity is reached at three points (i.e. at 7 m, 9.5 m and 11.5 m depth) indicating locations of shear failure. The behavior of the pile at 9.5 and 11.5 m depth is similar to this observed in the previous case. At 7 m depth though, after the shear failure the drift continues increasing and the shear force following the backbone curve starts degrading and eventually reaches the residual shear capacity. At this point axial failure is imminent.

6 CONCLUSIONS

A preliminary investigation of the post-failure axial capacity of poorly reinforced piles has been carried out using a developed methodology/approach based on the research findings of Elwood and Moehle (2003) who examined the residual axial capacity of lightly reinforced columns that are prone to fail in shear. Analysis of a case study from northern Europe have shown that poorly-reinforced piles can bear vertical loads even after shear failure has initiated, as long as the imposed drifts on the pile are less than a critical value. Given the seismic demand in the area, for most of the cases analyzed, the pile fails in shear, but it seems that it can continue bearing the vertical loads. Although the development of the proposed approach lies on solid scientific evidence, inevitably, application of Elwood and Moehle (2003) model to piles includes several assumptions and hypotheses that require experimental verification. Main assumptions of the developed methodology as presented in this paper to be verified include the extrapolation of model application from columns to piles and the contribution of the central rebar to the shear resistance of the crosssection. This paper is about single structural pile performance. It is important to note that seismic assessments of global building response consider the full foundation system, including all piles and (partial) embedded foundation beams. The full building-foundation-soil system should be analyzed to ensure that all force and shear resisting components and load retribution effects are taken into account and to arrive at a representative individual seismic pile loading regime.

REFERENCES

American Petroleum Institute (2000) "Recommended Practice for Planning, Designing, and Constructing Fixed Offshore Platforms," RP 2AWSD, 21st Edition, API, Washington, D.C., December.

Darendeli, M. (2001) Development of a new family of normalized modulus reduction and material damping curves. *Ph.D. Thesis*, Dept. of Civil Eng., Univ. of Texas, Austin.

Elwood, K., and Moehle, J. P., (2003) Shake Table Tests and Analytical Studies on the Gravity Load Collapse of Reinforced Concrete Frames, PEER Report 2003/01, Pacific Earthquake Engineering Research Center, University of California.

EPPO (2012) Code of Structural Interventions 2012, GG 42/B/20-01-2012, Earthquake Planning and Protection Organization, Athens, Greece.
Lowes, L.N., Mitra, N., and Altoonash, A. (2004) A Beam-Column Joint Model for Simulating the Earthquake Response of Reinforced Concrete Frames, PEER Report 2003/10, Pacific Earthquake Engineering Research Center, University of California.
Maki, T. and Mutsuyoshi, H. (2004) "Seismic Behavior of Reinforced Concrete Piles under Ground". Journal of Advanced Concrete Technology, 2(1), pp. 37–47.
Mazzoni, S., McKenna, F., Fenves, G.L. (2010) OpenSees Online Documentation, http://opensees.berkeley.edu/wiki/index.php/Main_Page, Pacific Earthquake Engineering Center, University of California.
Mohammed, A.Y.M. and Maekawa, K. (2012) "Global and Local Impacts of Soil Confinement on RC Pile Nonlinearity Global and Local Impacts of Soil Confinement on RC Pile Nonlinearity". Journal of Advanced Concrete Technology, 10. pp. 375–388.
Rasmussen, H.B. (1963) "Resistance of Embedded Bolts and Dowels Loaded in Shear", BygningsstatiskeMeddelelser, Vol.34(2).
Sezen, H., (2002) Seismic Response and Modeling of Reinforced Concrete Building Columns, Ph.D. Dissertation, Department of Civil and Environmental Engineering, University of California, Berkeley.
Shirai N., Moriizumi, K., and Terasawa, K., (2001) Cyclic Analysis of Reinforced Concrete Columns: Macro-Element Approach, Modeling of Inelastic Behavior of RC Structures under Seismic Load, American Society of Civil Engineers, Reston, Virginia, pp. 435–453.
Yoshimura, M., and Yamanaka, N., (2000) Ultimate Limit State of RC Columns, Second US-Japan Workshop on Performance-Based Earthquake Engineering Methodology for Reinforced Concrete Building Structures, Sapporo, Japan, PEER report 2000/10. Berkeley, Calif.: Pacific Earthquake Engineering Research Center, University of California, pp. 313–326.